Mapping Large Regions of Diblock Copolymer Phase Space by Selective Chemical Modification

Drew A. Davidock,‡ Marc A. Hillmyer,*,† and Timothy P. Lodge*,†,‡

Department of Chemistry and Department of Chemical Engineering and Materials Science, University of Minnesota, Minneapolis, Minnesota 55455

Received August 22, 2003; Revised Manuscript Received October 30, 2003

ABSTRACT: A series of 4,1-polyisoprene-*b*-1,2-polybutadiene diblock copolymers of differing molecular weights and compositions were prepared by anionic polymerization. The polybutadiene blocks were selectively hydrogenated to poly(ethylethylene) using a homogeneous ruthenium catalyst. The double bonds in the polyisoprene blocks were subsequently modified to varying extents by the addition of difluorocarbene. The precursor polyisoprene−poly(ethylethylene) materials were disordered, but upon difluorocarbene (CF_2) addition the effective degree of segregation in these materials increased markedly. Small-angle X-ray scattering was used to characterize the ordered state morphologies and domains spacings. Effective interaction parameters (χ_{eff}) were extracted from the temperature- and composition-dependent domain spacings, and these in turn were used to place the various samples on an experimental segregation vs composition phase map. The interaction parameter between poly(ethylethylene) and polyisoprene increases by a factor of 370 upon complete CF_2 modification. This large enhancement enables examination of a much wider range of segregation strength than is accessible by varying temperature. A notable feature of these results is that the gyroid phase appears to be stable into the strong segregation regime, in contrast to expectations based on self-consistent-field theory.

Introduction

A quantitative understanding of block copolymer morphology maps or phase diagrams is central to the study of block copolymer thermodynamics and dynamics. A block copolymer phase diagram gives the equilibrium morphology of the system as a function of both the volume fraction of block *i*, f_i, and the degree of segregation, χN, where χ is the Flory−Huggins interaction parameter and N is the total degree of polymerization. In controlled synthesis schemes, both N and f_i can be readily varied. In contrast, χ is largely dictated by the selection of the monomers. Although the magnitude of χ can be tuned through its (typically inverse) relation to temperature, the range is usually limited in practice to a factor of 2−3. For example, χ for a polystyrene-*b*-polyisoprene increases only by a factor of 2 between 225 and 25 °C (from ca. 0.04 to 0.09).[1] Furthermore, issues of chemical stability at high temperature and the intervention of the glass transition or crystallization at low temperature also serve to limit the accessible range of χ.

Traditionally, the synthesis of a large number of block copolymers varying in both N and f_i is required to map the phase diagram adequately. Post-polymerization chemical modification of a parent copolymer can be a powerful tool for reducing the number of required parent materials. By selectively changing the chemical nature of one or both segments of a block copolymer, χ can be methodically varied over a large range (e.g., by over 2 orders of magnitude in the system described here). With appropriate design and control of the chemical modification(s), a single parent polymer could be used to explore the phase behavior from the weak segregation limit (WSL),[2] through the intermediate segregation regime (ISR)[3] and into the strong segregation limit (SSL);[4] the postulated super-strong segregation regime (SSSR) might also be accessible.[5,6] Important criteria for the chosen modification scheme(s) include the ability to generate substantial changes in χ, the ease of performing the modification and controlling its extent, and the ability to preserve the narrow molecular weight distribution of the parent material.

Polydienes and polydiene-containing block copolymers are appealing materials for modification because the double bond provides a versatile reactive site. Many modification chemistries, such as hydrogenation,[7,8] epoxidation,[9,10] hydrosilylation,[11] sulfonation,[12,13] chlorination,[14] and fluorination,[15−17] have been reported. Fluorination of polymers usually yields materials with high thermal and chemical stabilities, low surface tensions, and low friction coefficients.[15] These appealing properties of fluorine incorporation, combined with the strong thermodynamic incompatibility between fluoropolymers and most other macromolecules, are predicted to have significant consequences on the self-assembly behavior of block copolymers.[18−20]

In this work, we use a mild, selective, and quantitative fluorination method[16] to selectively insert difluorocarbene into the polydiene backbone of a series of 4,1-polyisoprene-*b*-poly(ethylethylene) (PI-*b*-PEE) diblock copolymers. The effect of both the extent of fluorination and temperature on the thermodynamic behavior of the blocks was determined in a quantitative manner, and χ was found to increase by a factor of approximately 370 upon complete modification. Using this information, the determination of the experimental phase diagram was carried out, and the results are compared with the theoretical diblock copolymer phase map constructed using self-consistent-field theory.[21] The most surprising result is the persistence of the gyroid phase into the strong segregation regime, which is in apparent conflict

† Department of Chemistry.
‡ Department of Chemical Engineering and Materials Science.
* Authors for correspondence: hillmyer@chem.umn.edu, lodge@chem.umn.edu.

10.1021/ma035248y CCC: $27.50
Published on Web 12/24/2003

Table 1. Molecular Characteristics of 4,1-PI-*b*-1,2-PB Diblock Copolymers

entry	10^3M_n[a]	PDI[a]	PDI[b]	10^3M_n[c]	10^3M_n[d]	f_{PB}[d]	sample code[f]	PI as 4,1- (%)[g]	PB as 1,2- (%)[g]
1	19.9	1.02	1.07	18.0	19.0	0.514	PIPB(9.4, 9.6)	94.4	94.7
2	19.1	1.01	1.05	19.0	19.1	0.464	PIPB(10.4, 8.7)	94.5	>99
3	10.3	1.03	1.07	8.8	9.5	0.499	PIPB(4.8, 4.7)	94.4	97.7
4	12.1	1.02	1.09	10.5	11.3	0.355	PIPB(7.1, 4.2)	94.3	98.6
5	11.2	1.02	1.08	9.8	10.5	0.345	PIPB(6.9, 3.6)	94.3	>99
6	12.3	1.01	1.07	11.4	11.8	0.284	PIPB(8.5, 3.3)	94.3	>99
7	12.2	1.01	1.06	11.2	11.7	0.210	PIPB(9.3, 2.4)	94.2	>99

[a] Measured by SEC equipped with a Wyatt MALS detector. [b] Measured by SEC based on PS standards. [c] Determined by end-group analysis from ^{1}H NMR spectra. [d] Average M_n of SEC and NMR results. [e] Determined from ^{1}H NMR spectra using room-temperature densities of ρ(4,1-PI) = 0.913 g/cm^3 and ρ(1,2-PB) = 0.889 g/cm^3.[31] [f] 4,1-PI-*b*-1,2-PB samples denoted as PIPB(*x*, *y*), where *x* and *y* represent the molecular weights of the PI block and PB block, respectively, calculated from mass percentages from ^{1}H NMR spectra. [g] Molar percents calculated from ^{1}H NMR spectroscopy.

with the calculations. A preliminary account of this phenomenon has been presented.[22]

Experimental Section

Materials. All chemicals were used without further purification except as noted. Isoprene (Aldrich) and butadiene (Aldrich) were purified by successive vacuum distillations from dibutylmagnesium followed by *n*-butyllithium, after stirring at 0 °C for 4 h in each case. Cyclohexane (Aldrich) was purified by passage through an activated alumina column (LaRoche) and a supported copper catalyst column (Engelhard). Degassed 1,2-dipiperidinoethane (DIPIP) (Sigma) was purified by stirring over CaH_2 for 48 h before vacuum distillation. Triethylamine (Aldrich) and methylene chloride (Aldrich) were both purified by passage through a column packed with activated alumina (Fisher). The concentration of *sec*-butyllithium (Aldrich) was determined by the Gilman double-titration method prior to use.[23]

Molecular Characterization. All block copolymers were characterized by size exclusion chromatography (SEC) and nuclear magnetic resonance (NMR) spectroscopy, after each step. The SEC system consisted of a Wyatt OPTILAB RI detector, a Wyatt Dawn multiangle light scattering detector (MALS), and three Phenogel (Phenomenex) columns with porosities of 10^3, 10^4, and 10^5 Å that were calibrated using polystyrene standards (Pressure Chemical Co.). The eluent was tetrahydrofuran (THF), and the samples (100 μL of 10 mg/mL) were injected with a flow rate of 1 mL/min. ^{1}H and ^{19}F NMR spectra were recorded on either a Varian Inova 300 or 500 MHz spectrometer. The NMR samples were prepared by dissolving approximately 25 mg of sample in 700 μL of deuterated chloroform (Cambridge Isotope Laboratories). For the ^{19}F NMR spectra, hexafluorobenzene (Aldrich) was added to the solutions as an internal standard ($\delta = -162.9$ ppm). Elemental analysis was performed on select samples by Galbraith Laboratories, Inc., of Knoxville, TN.

Synthesis of Block Copolymers. Seven 4,1-polyisoprene-*b*-1,2-polybutadiene (4,1-PI-*b*-1,2-PB) samples were synthesized by living sequential anionic polymerization using an established air- and water-free approach.[24] A brief description of a representative polymerization (entry 4 in Table 1) is given below. A 2 L round-bottom flask fitted with five internal ACETHREDS ports was heated to 270 °C at <30 mTorr for 12 h to remove adsorbed H_2O. After cooling to room temperature, purified cyclohexane (1 L) was added to the reactor and heated to 30 °C. A calculated aliquot of *sec*-butyllithium (1.03 M in cyclohexane, 11.36 mL, 11.6 mmol) was injected into the reactor followed by the immediate addition of purified isoprene (83.0 g, 1.22 mol). The reaction mixture was heated to 40 °C and stirred for 4 h. A small aliquot of the first block was removed and quenched with methanol for analysis. The temperature was lowered to 10 °C, and five equivalents relative to the lithium concentration of purified DIPIP (12.48 mL, 58.2 mmol) were injected as a polar modifying agent. The purified butadiene (46.8 g, 0.867 mol) was slowly added, and the reaction mixture was warmed to 18 °C and stirred for 3 h. These reaction conditions yield a polybutadiene block with very high 1,2-content.[25] The reaction was terminated by the injection of degassed methanol. The polymer was recovered by precipitation into a 1:1 2-propanol and methanol mixture and subsequently dried under vacuum (<30 mTorr) at RT for 96 h. The isolated yield was 126.7 g (97.6%). From the ^{1}H NMR spectrum, the 4,1-content of the PI and the 1,2-content of PB were determined to be 94.3% and 98.6%, respectively. The SEC analysis yielded a polydispersity index (PDI) of 1.02 by light scattering and 1.09 based on polystyrene (PS) standards. The number-average molecular weight (M_n) was calculated to be 12.1 kg/mol by SEC/MALS (Wyatt DAWN), which is close to the targeted molecular weight (M_n = 11.2 kg/mol) expected from reaction stoichiometry. All samples were stored at −20 °C.

Table 2. Molecular Characteristics of Selectively Hydrogenated Diblock Copolymers

entry[a]	initial PDI[b]	sample code[c]	PB conv (%)[d]	PI conv (%)[d]	fractionated PDI[e]
1	1.19	PIPEE(9.4, 10.0)	98.7	1.4	1.08
2	1.09	PIPEE(10.4, 9.0)	98.2	4.1	1.05
3	1.10	PIPEE(4.8, 4.9)	97.6	1.9	1.06
4	1.17	PIPEE(7.1, 4.4)	>99	1.4	1.08
5	1.09	PIPEE(6.9, 3.7)	>99	1.6	1.06
6	1.09	PIPEE(8.5, 3.4)	98.0	2.1	1.05
7	1.10	PIPEE(9.3, 2.5)	>99	1.6	1.06
8[f]	N/A	PIPEE(7.8, 3.9)	>98.5	2	1.06

[a] Entries correspond to same entries listed in Table 1. [b] PDIs of selectively hydrogenated material measured by SEC based on PS standards. [c] 4,1-PI-*b*-PEE samples denoted as PIPEE(*x*, *y*), where *x* and *y* represent the molecular weights of the PI block and PEE block, respectively, calculated from precursor block masses and extent of saturation. [d] Molar percents calculated from ^{1}H NMR spectroscopy. [e] PDIs of fractionated samples measured by SEC based on PS standards. [f] Entry 8 is composed of a 50:50 blend of fractionated samples of entries 4 and 6.

Selective Hydrogenation. Each of the 4,1-PI-*b*-1,2-PB block copolymers was subjected to a selective hydrogenation to convert the 1,2-PB block into poly(ethylethylene) (PEE) using a homogeneous ruthenium catalyst.[26,27] A representative example (entry 4 in Table 2) is given here. The 4,1-PI-*b*-1,2-PB copolymer (21.5 g, with a PI block of 7.1 kg/mol and PB block of 4.2 kg/mol, 198.7 mmol of PI and 148.0 mmol of PB olefinic sites) was dissolved in purified methylene chloride (860 mL) and sparged with dry nitrogen for 15 min. Under an argon atmosphere, dichlorotris(triphenylphosphine)ruthenium(II) (Strem) (2.12 g, 2.21 mmol) and a magnetic stir bar were added to a 1 L round-bottom flask and capped with a rubber septum. The polymer solution was added to the catalyst by cannulation, followed by the injection of purified triethylamine (0.62 mL, 4.42 mmol). The reaction mixture was sparged with dry nitrogen for 20 min. The hydrogenation was performed by supplying the reaction mixture with a slight positive pressure of hydrogen via a mineral oil bubbler for 96 h, during which the reaction mixture changed from a brown/black to a deep red/purple color. Upon completion, the Ru catalyst was removed from the solution by adding tris(hydroxymethyl)-phosphine (2.74 g, 22.10 mmol) (Strem) and allowing the solution to stir under a dry nitrogen atmosphere for 12 h. This

water-soluble phosphine ligand binds to ruthenium and can be removed by washing with water and passage through a column packed with silica gel (EM Science).[28] The polymer was isolated by precipitation into methanol and dried under vacuum (<30 mTorr) at RT for 72 h. The isolation yield was 20.9 g (96%). Characterization of the sample by ^{1}H NMR spectroscopy showed essentially complete saturation of the PB block (>99 mol %) with little saturation of the PI block (<1.4 mol %). SEC analysis yielded a polydispersity index of 1.17 based on PS standards. The broadening is due to a small shoulder that appears at lower elution volumes, possibly due to some chain coupling.

Fractionation. Standard fractionation techniques were used to remove higher molecular weight chains from the desired material. A representative example (entry 4 in Table 2) is presented here. The selectively hydrogenated polymer (18.9 g) was dissolved in toluene (945 mL) (Aldrich) at RT. Methanol (Aldrich) was slowly added until the solution became turbid. The mixture was heated to 50 °C and became transparent. More methanol was added until the solution once again just reached its point of turbidity. The polymer solution was then immediately transferred to an insulated separatory funnel and allowed to cool overnight. Upon complete cooling, the solution had phase separated into two layers, the bottom layer rich with the coupled chains and the top layer containing the desired product. Each layer was concentrated by rotary evaporation, precipitated into methanol, and dried in a vacuum (<30 mTorr) for 48 h at RT. The recovered yield was 13.9 g (73.4%) from the top layer and 4.8 g (25.3%) for the bottom layer. SEC analysis of the polymer recovered from the top layer revealed a single peak with a PDI of 1.08 based on PS standards. All samples were stored at −20 °C.

Difluorocarbene Reaction. The unsaturated PI block in the PI-*b*-PEE block copolymer was modified by the addition of difluorocarbene (CF_2) into the polymer backbone.[16,29] The fluorinations were carried out in cyclohexane using hexafluoropropylene oxide (HFPO) as the CF_2 source; a representative example is given here. The PI-*b*-PEE copolymer (1.1 g, with a PI block of 7.1 kg/mol and PEE block of 4.4 kg/mol, 9.99 mmol of PI olefinic sites) was dissolved in purified cyclohexane (200 mL) and sparged with argon for 20 min. The polymer solution was transferred to an evacuated high-pressure reactor containing a magnetic stir bar by cannulation. A known amount of HFPO (4.98 g, 30.0 mmol) was added to the reactor and heated to 180 °C for 4 h. After cooling to RT, the reactor was vented to an aqueous NaOH solution. The solution inside was filtered and precipitated into a 1:1 2-propanol:methanol mixture. The recovered polymer was subsequently vacuum-dried (<30 mTorr) at RT for 24 h and were further annealed at approximately 75 °C for at least 24 h. The isolated yield was 1.55 g (97%). SEC analysis yielded a monodisperse peak with a PDI of 1.09 based on PS standards. All samples were stored at −20 °C.

Blend Preparation. Blends of the selectively hydrogenated PI-*b*-PEE precursors were prepared by codissolution of the fractionated samples in cyclohexane before subjecting them to the CF_2 modification described above. Some blends of the fluorinated polymers with similar extents of CF_2 modification were also prepared by codissolution in methylene chloride, followed by evaporation of the solvent under nitrogen and drying in a vacuum (<30 mTorr) for 24 h at RT and for 24 h at 75 °C.

Solvent-Cast Films. Dilute polymer solutions (10 wt %) were prepared gravimetrically and cast onto glass watch plates. The solvent was allowed to slowly evaporate for 24 h under a nitrogen atmosphere, and the resulting films were subsequently dried under vacuum (<30 mTorr) at RT for at least 24 h to ensure complete removal of the solvent.

Small-Angle X-ray Scattering (SAXS). SAXS measurements were made on the University of Minnesota 2 m beamline. Copper Kα X-rays with a wavelength of 1.542 Å were generated by a Rigaku RU-200BVH rotating anode and fitted with a 0.2 × 2 mm microfocus cathode. Franks mirror optics were used to focus the beam onto a two-dimensional (2-D) Siemens multiwire area detector. The 2-D images were corrected for detector response, azimuthally integrated, and shown as 1-D plots of intensity vs wave vector (q). Sample temperatures were controlled using a thermostated brass block contained inside an evacuated sample chamber. Exposure times ranged from 5 to 30 min at a given temperature, and samples were annealed for at least 5 min at a given temperature prior to measurement.

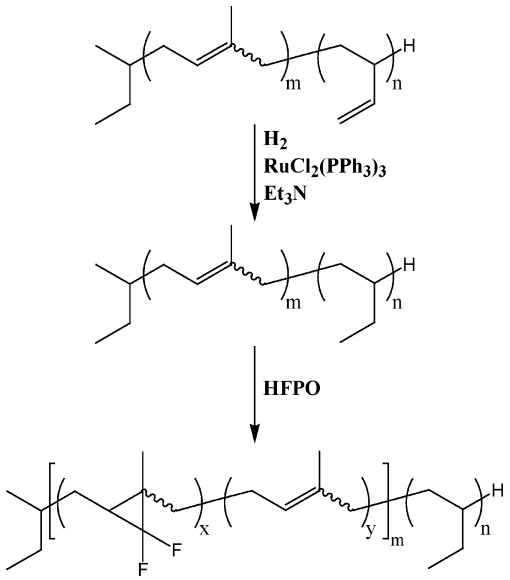

Figure 1. Schematic illustration for the selective hydrogenation of the 1,2-PB block in 4,1-PI-*b*-1,2-PB copolymers into PEE and subsequent difluorocarbene modification of the PI block.

Small-Angle Neutron Scattering (SANS). SANS samples were made by first preparing four dilute solutions (10%) of PIPEE(7.1, 4.4)F100 gravimetrically, two in protonated acetone and two in deuterated acetone (*h*- and *d*-acetone, respectively). The solvent was allowed to slowly evaporate under nitrogen until concentrations (ϕ) of 50% and 75% polymer were obtained for both solvents. The mixtures were transferred to the SANS cells, consisting of two quartz disks (1 in. diameter) separated by a 1 mm thick aluminum ring with an inner diameter of 15 mm. The system was sealed with high-temperature silicone adhesive (General Electric). The cells were subsequently annealed at 40 °C for 48 h. SANS measurements were performed at the National Institute of Standards and Technology Cold Neutron Research Facility on the NIST/Exxon/University of Minnesota 30 m instrument (NG-7). The neutrons had a wavelength of 6 Å and a resolution of $\Delta\lambda/\lambda = 0.11$. The samples were maintained at 30 °C, and the sample-to-detector distance was 7 m. Exposure times were 10 min. The data were corrected for detector sensitivity, background, and empty cell scattering and were azimuthally averaged and placed on an absolute scale using the direct beam method. The 2-D data were converted to the 1-D form of intensity vs wavevector.

Results

We prepared a series of PI-*b*-PEE block copolymers by the selective hydrogenation of the PB block in 4,1-PI-*b*-1,2-PB block copolymers. These materials were then subjected to subsequent difluorocarbene modification of the PI block as shown in Figure 1. In this section, we describe the synthesis and characterization of the precursor and modified block copolymers.

Synthesis of Parent Block Copolymers. The general synthetic procedure used to prepare 4,1-PI-*b*-1,2-PB was reported by Bates et al.[30] The 4,1-PI-*b*-1,2-PB precursor block copolymers used in this study are listed in Table 1. The samples are designated as PIPB(x, y), where x and y are the molecular weights in kg/mol of the PI and PB blocks, respectively. Entries 1 and 2 are

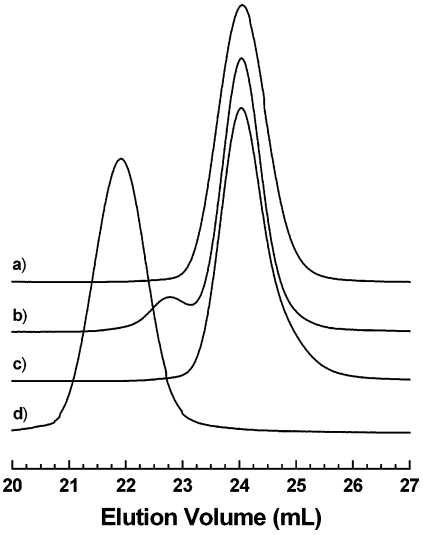

Figure 2. SEC traces of a representative 4,1-PI-*b*-1,2-PB after each procedural step: (a) 4,1-PI-*b*-1,2-PB precursor block copolymer; (b) 4,1-PI-*b*-PEE; (c) fractionated 4,1-PI-*b*-PEE; (d) fully difluorocarbene modified FPI-*b*-PEE sample.

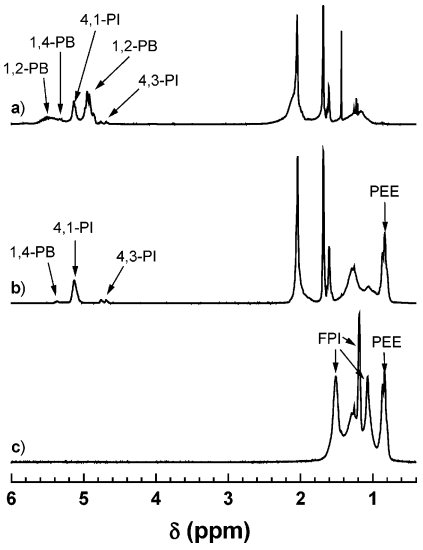

Figure 3. ^{1}H NMR spectra of a representative sample after each procedural step: (a) 4,1-PI-*b*-1,2-PB precursor block copolymer; (b) 4,1-PI-*b*-PEE (notice disappearance of 1,2-PB); (c) fully difluorocarbene modified FPI-*b*-PEE sample showing disappearance of all olefin peaks.

larger molecular weight (~19 kg/mol), symmetric polymers, and entries 3−7 are lower molecular weight (~11 kg/mol) samples with varying volume fractions ($f_{PB} \approx 0.50-0.21$). The diblocks all have narrow, monomodal molecular weight distributions as determined by SEC (Figure 2a). The molecular weights shown in Table 1 represent an average of those determined by SEC/LS and those calculated from end-group analysis of the ^{1}H NMR spectra assuming one *sec*-butyl group per polymer. Both are in good agreement with the targeted molecular weight estimated from reaction stoichiometry. The ^{1}H NMR spectra (see Figure 3a for a representative example) were used to determine the polydiene microstructures and compositions from the ratios of the signals in the olefinic region (5.6−4.6 ppm). All samples have 4,1-PI contents of ~94% and very high 1,2-PB content (94−100%). A very high vinyl content in the PB block is essential for the subsequent selective hydrogenation step.

Selective Hydrogenation of the PB Block. The reactivity of alkenes is typically dependent upon the degree of alkene substitution,[32] and therefore the unsubstituted double bond of 1,2-PB vs that of 4,1-PI can be selectively hydrogenated to yield PEE. The result is a saturated block that should be more chemically inert and resistant to further modification. Chlorotris(triphenylphospine)hydridoruthenium(II) ($(Ph_3P)_3RuClH$) has been used to selectively saturate the vinyl group of small organic molecules in the presence of other alkenes.[33−35] This catalyst can also be used to selectively hydrogenate the pendant double bonds of 1,2-PB.[26,27] This active catalytic species was generated in situ from dichlorotris(triphenylphosphine)ruthenium(II) ($(Ph_3P)_3RuCl_2$) and triethylamine. Once the hydrogen feed to the reaction mixture was stopped, it became a dark green color, and removal of the catalyst from the desired product was accomplished using a water-soluble phosphine ligand ($P(CH_2OH)_3$)[28] and confirmed by elemental analysis (>97.0% Ru and >97.6% P removal).

Table 2 lists the molecular characteristics of the PI-*b*-PEE block copolymers, and each entry corresponds to the precursor 4,1-PI-*b*-1,2-PB block copolymer listed in Table 1 with the same entry number. The hydrogenated samples are designated in a manner similar to the precursors. By SEC, all samples were found to have a monodisperse main peak and a small shoulder or peak at lower elution volumes as illustrated in Figure 2b. This high molecular weight material has approximately twice the molecular weight of the main peak and is presumably due to a small amount of chain coupling. Fractionation was used to remove the high molecular weight material, as shown in Figure 2c, and this gave materials with narrow polydispersity indices (PDIs) similar to those of the polydiene precursors. Comparison of the SEC results for the precursor and selectively hydrogenated diblock copolymers shows that the peaks occur at approximately the same elution volumes, indicating that the hydrodynamic volume does not change significantly. Extents of hydrogenation of both the PI and PB blocks were determined by ^{1}H NMR spectroscopy. As indicated in Figure 3b, the saturation of PB was confirmed by the disappearance of the 1,2-PB olefin resonances (5.5, 5.0 ppm) and the appearance of an aliphatic $-CH_3$ group peak (0.9 ppm). Incomplete hydrogenation of the PB block is usually due to the presence of a small amount of 1,4-PB which is not saturated as efficiently. For each sample, a small amount of PI block saturation was obtained with nearly complete saturation of the PB block (see Table 2). The ^{1}H NMR spectra were virtually identical for the materials before and after fractionation, indicating that the coupling reaction did not significantly impact the level of hydrogenation.

Addition of Difluorocarbene to the PI Block. Fluorination of the PI was accomplished by the in situ generation and insertion of difluorocarbene from HFPO into the PI backbone in a manner similar to that described elsewhere.[16,29] The extent of CF_2 modification was controlled by varying the reaction time and/or the stoichiometric ratio of HFPO to olefinic sites in the PI block. The fluorinated samples are designated as PIPEE-(*x*, *y*)F*z*, where *x* and *y* are the molecular weights (in kg/mol) of the PI and PEE blocks of the hydrogenated precursor, respectively, and *z* represents the molar percentage of PI repeat units that have been modified with difluorocarbene.

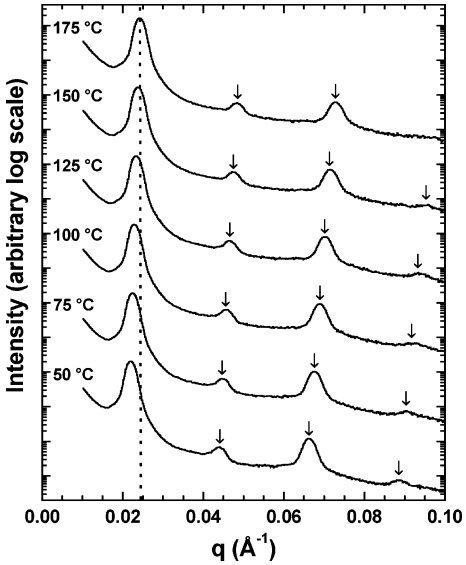

Figure 4. One-dimensional SAXS profiles for PIPEE(10.4, 9.0)F100 at different temperatures. The arrows correspond to the positions with integral multiples of q^*. The data were shifted vertically for clarity.

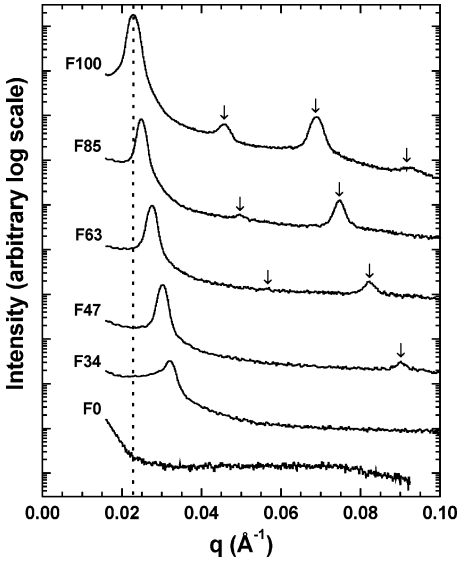

Figure 5. One-dimensional SAXS profiles at 100 °C of a series of PIPEE(10.4, 9.0)F*z* with different degrees of CF_2 modification (*z*). The arrows correspond to the positions with integral multiples of q^*. The data were shifted vertically for clarity.

All CF_2-modified samples used in this study had similar PDIs and peak shapes by SEC as the hydrogenated precursors from which they were derived. This indicates that no significant chain scission or coupling occurred during the modification, consistent with previous reports.[16,29] As the level of CF_2 modification increases, the peak shifts to lower elution volumes, as shown in Figure 2d, corresponding to an increase in hydrodynamic volume. The extent of CF_2 insertion was calculated from the ^{1}H NMR spectra of the modified samples. A representative spectrum of a completely modified sample demonstrating the disappearance of all olefin peaks is shown in Figure 3c.

Morphological Characterization. SAXS was used to study the effects of temperature (T), extent of CF_2 modification (F*z*), and composition (f_{PEE}) on the self-assembly behavior of the PIPEE(*x*, *y*)F*z* samples. All samples were annealed for a minimum of 24 h at 75 °C and measured at temperatures greater than that of the highest T_g component ($T_{g,FPI} \approx 43$ °C).[16] To ensure equilibration, many of the samples were further annealed for up to 3 weeks at elevated temperatures (~120 °C) and reevaluated by SAXS. Negligible differences in the scattering profiles were obtained, so we infer that all samples are at equilibrium.

Figure 4 shows SAXS profiles for the fully modified PIPEE(10.4, 9.0)F100 at selected temperatures. A sharp principal scattering peak at wavevector q^* and several higher-order peaks were consistently observed. The integral ratios of these higher-order peak wavevectors to q^* demonstrate that these samples have a lamellar morphology. The position of the principal peak steadily shifts to lower q values as the temperature is decreased. From the relationship

$$D = \frac{2\pi}{q^*} \tag{1}$$

the experimental domain spacing (D) of these block copolymers can be determined. Hence, decreasing the temperature leads to an increase in domain spacing, consistent with an increasing degree of segregation between the blocks.

Figure 5 shows SAXS scattering profiles for a series of fluorinated copolymers prepared from the same precursor, PIPEE(10.4, 9.0), at 100 °C. There is insufficient electron contrast between the PI and PEE blocks for reliable SAXS analysis, but the material is expected to be disordered since the components of the original parent material, 4,1-PI and 1,2-PB, have been shown to be miscible,[36−41] and the hydrogenation is predicted to cause a very modest increase in χ since most polydiene or polyolefin pairs display only slight incompatibilities ($\chi \leq 0.01$).[42,43] As the extent of CF_2 modification was increased (F34), a sharp primary peak developed as sufficient electron contrast was reached, and the material was ordered. Upon further CF_2 addition, higher-order reflections were observed, demonstrating that the sample is becoming increasingly segregated. The ratio of these higher-order peak positions to the principal scattering peak corresponds to a lamellar structure, consistent with the expected morphology since the volume fraction of the PEE block (f_{PEE}) decreases only slightly from 0.478 for the unfluorinated sample (PIPEE(10.4, 9.0)F0) to 0.421 for the fully modified sample (PIPEE(10.4, 9.0)F100). Also, there is a large increase in D with increasing CF_2 modification since the position of the principal peak moves to lower q, consistent with an increasing degree of segregation.

Morphologies other than L were obtained at lower values of f_{PEE}.[22] This transformation was observed by SAXS on the basis of the ratios of the peak spacings. Entries 1−4 in Table 2 always exhibited L and entries 6 and 7 consistently were C. Entry 5 has a lamellar morphology at low and moderate extents of CF_2 modification, but above $z \approx 85$, the morphology changes to G.[22] Entry 8, the blend, was also found to exhibit G consistently.[22]

To investigate the equilibrium nature of the observed gyroid phase, PIPEE(7.8, 3.9)F100, PIPEE(6.9, 3.7)-F100, and PIPEE(6.9, 3.7)F92 were cast into thin films from a number of solvents with various selectivities.[22] The cast morphology was determined by SAXS. The samples were annealed in the beamline at 150 °C and scanned every hour for up to 4 h to determine whether the G phase was recovered. If no observable change in

Table 3. Cast and Annealed Morphologies from Various Solvents

sample	solvent	δ (MPa$^{1/2}$)[a]	cast morphology[b]	annealed morphology[b]	total annealing time
PIPEE(7.8, 3.9)F100	hexanes	14.9	L	G	1 h
	α,α,α-trifluorotoluene	17.4	C	G	3 weeks
	chloroform	19.0	?→C	G	3 weeks
	methylene chloride	19.8	?→C	G	3 weeks
	1,2-dichloroethane	20.1	?→C	G	3 weeks
	dichlorobenzene	20.5	?→C	G	3 weeks
PIPEE(6.9, 3.7)F100	hexanes	14.9	L	G	1 h
	α,α,α-trifluorotoluene	17.4	L	G	1 h
	chloroform	19.0	L	G	3 h
	methylene chloride	19.8	L	G	3 h
	1,2-dichloroethane	20.1	L	L and G	4 h
	acetone	20.3	L	L and G	4 h
	dichlorobenzene	20.5	L	G	2 h
	acetonitrile	24.3	L	L and G	4 h
PIPEE(6.9, 3.7)F92	hexanes	14.9	L	G	1 h
	α,α,α-trifluorotoluene	17.4	L	L and G	4 h
	chloroform	19.0	L	L and G	4 h
	methylene chloride	19.8	L	L and G	4 h
	1,2-dichloroethane	20.1	L	L and G	4 h
	acetone	20.3	L	L and G	4 h
	dichlorobenzene	20.5	L	L and G	4 h
	acetonitrile	24.3	L	L and G	4 h

[a] Solubility parameters taken from ref 44. For the respective polymers, $\delta_{PEE} \approx 14-16$ MPa$^{1/2}$ and $\delta_{FPI} \approx 20-22$ MPa$^{1/2}$. [b] Morphologies determined by SAXS.

the scattering profiles was observed after 4 h, the samples were annealed in a vacuum oven (<30 mTorr) at 130 °C and reexamined by SAXS weekly to see whether G was recoverable. Table 3 lists the casting experiment results. PIPEE(7.8, 3.9)F100 cast into L from hexanes and C from all of the other solvents. A weakly ordered scattering profile inconsistent with any of the commonly observed morphologies was initially obtained from the PIPEE(7.8, 3.9)F100 cast from chloroform, methylene chloride, 1,2-dichloroethane, and dichlorobenzene, but after 5 min of annealing at 150 °C, a strong scattering profile consistent with C was obtained. The morphology gradually reverted to G with annealing at elevated temperatures with full recovery of G obtained after 3 weeks. PIPEE(6.9, 3.7)F100 and PIPEE(6.9, 3.7)F92 always cast into L regardless of the solvent. Upon annealing, G was found to recover in a matter of hours for all samples cast into L. For the L samples that took more than 1 h to anneal back to G, a coexistence of L and G was observed with the L peak(s) decreasing and G increasing in scattered intensity after each hour.[22] It is therefore reasonable to infer that those samples listed in Table 3 that exhibit coexistence of L and G would anneal completely to G eventually.

Discussion

The primary purpose of this section is to obtain some insight into the effect of difluorocarbene modification on the self-assembly behavior of these block copolymers. This can be done in a semiquantitative manner by obtaining estimates of the interaction parameter (χ) from the domain spacing (D).[29,45−47] The equilibrium domain spacing is determined by balancing the unfavorable interfacial energy between the incompatible A and B domains and the entropic penalty due to the stretching of the polymer coils so as to maintain a uniform segment density.[48−52] Semenov showed that when these two terms are balanced, the microdomain period (D) scales as

$$D \sim \bar{a} N^{2/3} \chi^{1/6} \tag{2}$$

for the three "classical" block copolymer morphologies (lamellae, cylinders, and spheres) where $\bar{a}$ is the average statistical segment length of the block copolymer and N is the overall degree of polymerization. The explicit result for lamellar samples is

$$D = 1.10 \bar{a} N^{2/3} \chi^{1/6} \tag{3}$$

which applies strictly to lamellar materials in the strong-segregation limit ($\chi N \geq 100$). Nonetheless, eq 3 provides a reasonable and internally consistent estimate of χ for all ordered structures over a range of segregation values.[53] For example, Matsen and Bates compared the results of eq 3 at different segregation values with D values calculated from self-consistent mean-field theory liberated from the usual approximations.[21] The results differ by about 20% when $\chi N = 10$, by 5% when $\chi N = 40$, and by only 1% when $\chi N = 100$. Also, as the domain spacing is expected to scale according to eq 2 for the various microstructures with only a slightly different prefactor, there are only small changes in D upon crossing phase boundaries; the resulting χ values for the C and G samples may include a systematic error of up to 40%. However, these results yield smaller χ values since the domain spacing is found to decrease when moving from L to G.[54,55]

Extraction of χ from D using eq 3 necessitates the investigation of the effect of the difluorocarbene modification on N and $\bar{a}$. The degree of polymerization, N, is based on a reference repeat unit volume and differs from the chemical degree of polymerization. In this study, a polystyrene (PS) repeat unit reference volume was chosen for comparison to the commonly studied PS-*b*-PI system. The extent to which N increases depends on f_{PEE}. Since the PEE block is unaffected by the difluorocarbene modification, N_{EE} does not change, and the change in N is due entirely to the change in $N_{I/FI}$. As the volume fraction of PEE in the block copolymer increases ($f_{PEE} \rightarrow 1$), the change in N with fluorination decreases. For example, for a series of PI-*b*-PEE copolymers, N increases upon complete difluorocarbene modi-

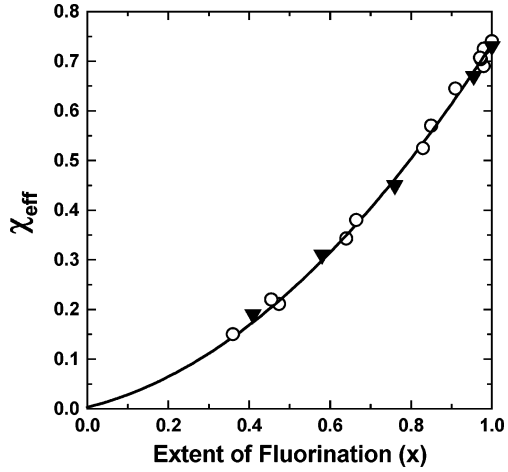

Figure 6. Dependence of the calculated χ_{eff} at 100 °C on the extent of difluorocarbene modification (x) on a volume basis. The open circles are for PIPEE(10.4, 9.0), and the solid triangles are for PIPEE(7.1, 4.4) (entries 2 and 4, respectively, in Table 2). The solid line is the best-fit quadratic curve for $y = ax^2 + bx + c$ with fitting coefficients of $a = 0.49$, $b = 0.24$, and $c = 0.0033$.

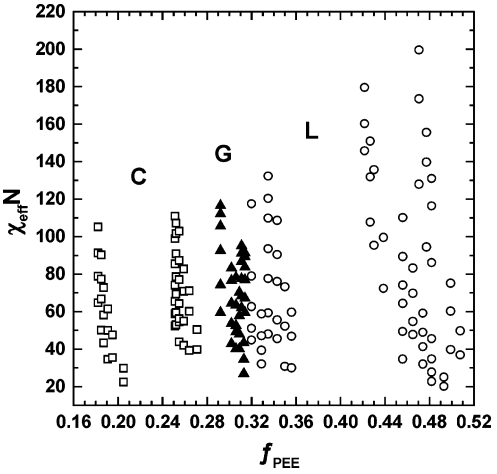

Figure 7. Experimental phase diagram for (PI-*stat*-FPI)-*b*-PEE obtained from the seven precursors and one blend by varying both the extent of fluorination and the temperature (50−200 °C). Data representations: open circles, lamellae; solid triangles, gyroid; open squares, cylinders.

fication by 25.7% when $f_{PEE} = 0$, by 18.8% when $f_{PEE} = 0.3$ initially, and by 11.2% when $f_{PEE} = 0.6$ initially. The appropriate average statistical segment length for a (PI-*stat*-FPI)-*b*-PEE copolymer ($\bar{a}_{IEE}$) is given by

$$\bar{a}_{FIEE} = \left(\frac{1 - f_{PEE}}{(1-x)a_I^2 + xa_{FI}^2} + \frac{f_{PEE}}{a_{EE}^2}\right)^{-1/2} \qquad (4)$$

where x is the extent of CF_2 modification of the PI block on a volume basis.[29] The average statistical segment length can be calculated using literature values of $a_{PI} = 7.6$ Å, $a_{FPI} = 7.3$ Å, and $a_{PEE} = 5.7$ Å (corrected to a PS reference volume using the room temperature densities of $\rho_{PS} = 1.04$ g/cm^3, $\rho_{PI} = 0.913$ g/cm^3, $\rho_{FPI} = 1.26$ g/cm^3, and $\rho_{PEE} = 0.869$ g/cm^3).[29−31,56,57] The statistical segment length has only a slight dependence on temperature, so we neglect this effect.[58] The average statistical segment length in fact turns out to be nearly constant, decreasing less than 1.8% upon complete CF_2 incorporation.

With the calculated N and $\bar{a}$ values and experimentally obtained D values, χ_{eff} values can be obtained for each sample using eq 3. Figure 6 shows the range of χ_{eff} values at 100 °C obtained from two lamellar samples (PIPEE(10.4, 9.0) and PIPEE(7.1, 4.4)) as a function of the level of difluorocarbene modification. To quantify this behavior, we employed a binary interaction model that was originally used to account for the phase behavior in a blend of a homopolymer of chemical repeat unit A and a statistical copolymer composed of two other repeat units (B-*stat*-C).[59−61] This is similar to our system, in which the PEE block acts as the homopolymer and the (PI-*stat*-FPI) block acts as the statistical copolymer. For such a three-component system, the effective interaction parameter of the system can be expressed in terms of the three pairwise interaction parameters and the composition of the statistical coblock as

$$\chi_{eff} = \chi_{FIEE}x + \chi_{IEE}(1 - x) - \chi_{IFI}x(1 - x) \qquad (5)$$

where χ_{FIEE}, χ_{IEE}, and χ_{IFI} are the pairwise interaction parameters among the fluorinated polyisoprene (FI), poly(ethylethylene) (EE), and polyisoprene (I) segments. This model fits the data very well (Figure 6), and the resulting values of the pairwise interaction parameters are $\chi_{FIEE} = 0.74$, $\chi_{IEE} = 0.002$, and $\chi_{IFI} = 0.49$ at 100 °C. Thus, χ is found to increase by a factor of ~370 going from F0 to F100 at this temperature.

The value between I and FI is in excellent agreement with the value of $\chi_{IFI} = 0.46$ at 100 °C found independently by Ren and co-workers in a PS-*b*-(PI-*stat*-FPI) copolymer.[29] The extremely small value obtained for the parent material (PI-*b*-PEE) was also expected, as discussed earlier, since 4,1-PI and 1,2-PB exhibit miscibility, and the hydrogenation is not expected to have a large effect.[36−43] Upon complete CF_2 modification, there is a significant increase in χ_{eff} resulting from the strong incompatibility between the hydrocarbon and fluorinated segments. Note that the large increase in χ reflects the fact that difluorocarbene is a polar moiety,[29] and thus the cohesive energy density of FPI is much larger than that of hydrocarbons.

The same approach as shown in Figure 6 was applied at other temperatures (50, 75, and 125 °C) and the three pairwise interaction parameters were determined in each case. Assuming the typical temperature dependence of χ[52]

$$\chi = \frac{\alpha}{T} + \beta \qquad (6)$$

where α and β are enthalpy and excess entropy coefficients, respectively, the temperature dependence of each pairwise interaction parameter was estimated. Substitution of these expressions into eq 5 leads to a single expression (eq 7) for calculating the χ_{eff} of this system at any temperature and extent of difluorocarbene incorporation.

$$\chi_{eff} = \left(\frac{383}{T} - 0.303\right)x + \left(\frac{14.3}{T} - 0.0353\right)(1 - x) - \left(\frac{139}{T} + 0.129\right)x(1 - x) \qquad (7)$$

Figure 7 shows the location of the data points on the experimental phase diagram based on the calculated compositions (f_{PEE})[62] and degrees of segregation ($\chi_{eff}N$)

obtained from the scattering profiles with the use of eq 3. All the data points were obtained from just the eight parent materials listed in Table 2 by varying the extent of CF_2 modification and/or the temperature. For the blend (entry 8, Table 2), comparable results were obtained whether two samples with similar levels of fluorination were blended together and measured or whether hydrogenated precursors were blended together, subjected to various levels of fluorination, and measured. For all samples, only those showing an ordered structure are shown. In other words, samples with low extents of fluorination ($x \lesssim 35$) are not shown because they are still in a disordered state, and thus no estimate of χ_{eff} could be obtained from this analysis procedure. The disordered state scattering profiles cannot yield an estimation of χ_{eff} due to the insufficient electron contrast between the blocks at low difluorocarbene levels. The phase diagram shows lamellae (L) and cylinder (C) phases separated by a narrow window of the bicontinuous gyroid phase (G).[22] The existence of these three phases and the location of their transitions between one another along the compositional axis are generally consistent with the results expected from theoretical phase diagram studies conducted by Matsen and Bates.[21,63] The slight shift and curvature of the phase boundaries are most likely due to the conformational asymmetry of the block copolymer ($a_{EE} \neq a_{I/FI}$).[64]

There are two prominent features in Figure 7. The first is the unprecedented large sweep in segregation values obtained by simply varying the extent of fluorination within each sample. The precursors are initially in a disordered state ($\chi N < 10.5$), but by the complete addition of difluorocarbene along the PI backbone, the materials all fall into the strong segregation regime ($\chi N > 100$). The second is the persistence of the G window at very large χN values.[22] This result is inconsistent with theory which anticipates that this complex phase should narrow and pinch off at a triple point with L and C at segregation values of approximately 60.[21]

The simplest possible explanation for the latter result is that the estimate of χ from eq 3 is substantially too large, but we do not believe this to be the case. When considering the G phase, we observe samples at segregation values twice that predicted by theory.[21] If the estimate of χ_{eff} was systematically high by a factor of 2, this would require that samples that we observe to be ordered at relatively low segregation values should actually be classified as disordered. Therefore, this hypothesis can be discarded. Separate measures of χ_{eff} were also determined from the order−disorder transition temperatures (T_{ODT}) from SAXS for two samples at low degrees of fluorination, PIPEE(4.8, 4.9)F33 with a lamellar morphology and PIPEE(9.3, 2.5)F34 with a cylinder morphology. The exact T_{ODT} values are not known, but they fall between 100 and 125 °C for both samples since ordered and disordered state scattering profiles were obtained at these temperatures, respectively. With the ODT temperatures, we can compare the experimentally determined χ_{eff} value with theoretically predicted values. Using fluctuation theory and the known values of N, we obtained $\chi_{fluc} = 0.124$ and 0.335 for the lamellar and cylinder samples, respectively.[65] The χ_{fluc} value for the lamellar sample is slightly lower than the experimentally predicted range of $0.160 > \chi_{exp} > 0.140$ obtained from eq 7 but is still in reasonable agreement. The experimental values of $0.167 > \chi_{exp} > 0.146$ for the cylinder samples are a factor of 2 smaller than the fluctuation theory's prediction, implying that, if anything, the χ_{eff} values used in Figure 7 could be too small. This difference is most likely due to the unaccounted for conformational asymmetry between the two blocks. Since $a_{PEE} < a_{PI/FPI}$, the theoretical phase diagram would be shifted to the left (lower f_{PEE}), resulting in a lower χN_{ODT} value and a more consistent χ_{eff} value.

Another possible explanation for the existence of the G phase at strong segregation is that the samples may not be at equilibrium. Preliminary results on the stability and equilibrium nature of the observed G phase in this system were presented in a previous work.[22] Long-term bulk annealing at elevated temperatures showed no change in the observed G morphology by SAXS. Casting of bulk G samples into L or C was performed using solvents of various selectivities. On the basis of other results and solubility tests performed on the respective homopolymers, PEE and FPI are expected to have solubility parameters of $\delta \sim 14-16$ and $20-22$ $MPa^{1/2}$, respectively.[29,44] Solvents with solubility parameters close to these values would be expected to preferentially swell that respective block. Films cast with PEE selective solvents are expected to shift f_{PEE} to the right resulting in films that are either L or G. Conversely, if the films are cast with FPI selective solvents, the expected cast morphology would be either C or G since f_{PEE} is expected to decrease. In all cases listed in Table 3, G was recovered from the cast morphology upon annealing. This is strong evidence that G is the equilibrium phase or at least is stable with respect to L and C. An unanticipated result is that L was consistently obtained as the cast morphology in PIPEE(6.9, 3.7)F100 and PIPEE(6.9, 3.7)F92. This was unexpected since solvents with $\delta \gtrsim 20$ $MPa^{1/2}$ were found to be good solvents for FPI but poor for PEE, so C or G were expected as the cast morphologies.

The origin of this anomaly has not been determined. Other experiments and calculations have shown that the substrate or surface can impact the orientation or morphology of a block copolymer due to favorable or unfavorable interactions with a specific component of the block copolymer.[66−71] Identical solutions in acetone were cast onto a number of different surfaces including a glass watchplate, a Teflon sheet, a silica wafer, an aluminum plate, and "Teflon-impregnated" aluminum plates. Identical scattering profiles consistent with the L morphology were obtained in each case, indicating that the substrate does not seem to be affecting the morphology. Another possibility is the preferential segregation of one block to the sample−air interface. This effect was observed by Wang and co-workers in other fluorinated materials due to the low surface energy density of the fluorinated blocks.[72]

To ensure that the acetone was swelling the FPI block as expected, SANS experiments were performed on solutions of the polymer in acetone. SANS experiments can be used to investigate whether there was preferential solvation or partitioning of the solvent (acetone) into one block, equal solvation of both blocks, and/or segregation of the solvent to the block interface. The results are only semiquantitative since the data could not be fully corrected for transmission as a result of a few residual air bubbles in the samples that could not be annealed out due to the low boiling point of acetone (56 °C). Only a brief explanation of the SANS analysis procedure for determining solvent distribution is pre-

Table 4. SANS Contrast Factors, $(b_\alpha - b_\beta)^2$, in Units of cm^{-1}

	PEE	FPI	*h*-acetone	*d*-acetone
PEE	0	0.0468	0.00562	0.540
FPI	0.0468	0	0.0200	0.269

sented here. A thorough description has been described elsewhere by Lodge and co-workers.[73]

The scattered intensity from the *j*th harmonic $I(jq^*)$ can be written as[74]

$$I(jq^*) = (b_{FPI} - b_{sol})^2\varphi_{FPI,j}^{\ 2} + (b_{PEE} - b_{sol})^2\varphi_{PEE,j}^{\ 2} + ((b_{FPI} - b_{sol})^2 + (b_{PEE} - b_{sol})^2 - (b_{FPI} - b_{PEE})^2)\varphi_{FPI,j}\varphi_{PEE,j} \quad (8)$$

where b_α and φ_α represent the scattering length density and the local deviation from the average concentration or composition, respectively, of component α. The quantities $(b_\alpha - b_\beta)^2$ represent the SANS contrast factors, and the calculated values referenced to a PS unit volume are presented in Table 4. The incompressibility assumption requires that

$$\varphi_{sol,j} + \varphi_{FPI,j} + \varphi_{PEE,j} = 0 \quad (9)$$

and if the solvent is uniformly distributed ($\varphi_{sol,j} = 0$), the scattered intensity profiles should be identical for the pair of solutions (*d*- and *h*-acetone) since the scattering length density of the solvent drops out of eq 8. As Figure 8 demonstrates, the scattering profiles for the *d*- and *h*-acetone solutions ($\phi = 0.75$, where ϕ represents the polymer volume fraction in the solutions) differ considerably with respect to the intensity of the primary peak, and thus the solvent is not uniformly distributed. On the basis of solubility tests of the homopolymers, the FPI domains should be preferentially swelled by acetone. The degree of solvation can be found by taking the ratio of the protonated and deuterated solvents' primary peak intensities according to eq 8. To eliminate one of the two unknowns, ($\varphi_{FPI,j}$, $\varphi_{PEE,j}$), we can assume that the solvent profile's first harmonic is proportional to that of the FPI component

$$\varphi_{sol,1} = \alpha\varphi_{FPI,1} \quad (10)$$

Substituting in the contrast factors and q^* intensities, α was found to have values of 0.21 and 0.44 for the $\phi = 0.75$ and 0.50 solutions, respectively. These positive values indicate that the solvent is significantly selective for FPI, as expected.

Another possibility to consider is that the apparent "misdirection" of the samples cast from FPI selective solvents into L may actually be a reasonable result. Extensive studies of copolymer solution phase behavior have shown that the effective position of a sample in the phase diagram can be shifted horizontally, vertically, or diagonally, depending on the concentration and selectivity of the solvent.[75,76] The two samples that appear to be "miscast" from FPI selective solvents, PIPEE(6.9, 3.7)F100 and PIPEE(6.9, 3.7)F92, sit just inside the G window in the bulk state near the G−L boundary. If the solvent were to substantially increase the segregation of the system, the dilution of the sample could move the location on the phase diagram almost vertically along the segregation axis and therefore back into L if the G−L boundary has some slight curvature to the left or if the G window does in fact possess an upper limit. This possibility is at least consistent with the observation that the scattering profiles for the cast L samples show a 15% increase in the domain size vs the C or G samples.

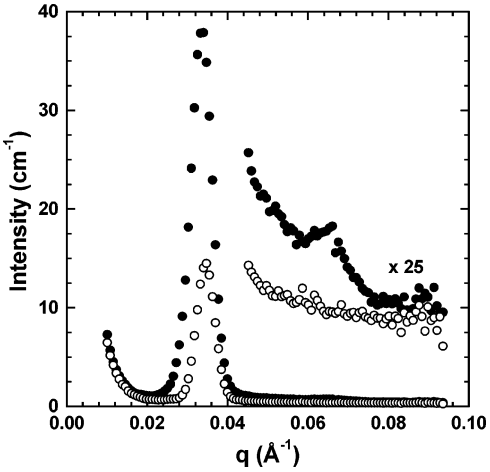

Figure 8. One-dimensional SANS profiles for PIPEE(7.1, 4.4)-F100 in *d*-acetone (solid circles) and *h*-acetone (open circles), $\phi = 0.75$, at 30 °C. The statistical error bars are comparable to the size of the points.

Finally, it is interesting to note that in all of these experiments the metastable hexagonally perforated layer (HPL) phase was never observed. Many experiments have shown HPL to be a metastable intermediate phase obtained when transforming between the L and G phases and also between C and G phases.[55,77−83] The HPL phase often forms because its layerlike structure helps to reduce the interfacial tension, thus facilitating the transformations in to and out of G.[51] The appearance of the HPL phase and the kinetics for the transformations between phases are usually affected by the depth of the quenches. For cylinder samples, direct transformations from C → G have been observed for shallow quenches.[83] This may explain why PIPEE(7.8, 3.9)F100 followed the expected casting trends by forming C from FPI selective solvents and why no HPL phase was observed during the anneal back to G. PIPEE(7.8, 3.9)-F100 is located much closer to the C−G boundary than the other two samples. Following the same trajectory argument introduced earlier, this sample could be expected to enter the C phase since it is much closer to that boundary. If it only slightly entered the C phase, it is comparable to a shallow quench so the lack of the intermediate HPL phase is perhaps not surprising.

Summary

We have prepared and characterized a set of (PI-*stat*-FPI)-*b*-PEE copolymers obtained from model 4,1-PI-*b*-1,2-PB copolymers by the selective hydrogenation of 1,2-PB into PEE followed by modification of the 4,1-PI with difluorocarbene. The morphologies and domain spacings at varying extents of CF_2 addition were determined by SAXS at various temperatures. Strong-segregation theory was used to obtain estimates for χ_{eff} between the PEE and partially CF_2-modified PI blocks. Upon complete fluorine modification, χ_{eff} was found to increase by a factor of 370 at 100 °C. This behavior can be explained by the introduction of a binary interaction model, which allows for the extrapolation of the pairwise interaction parameters. We found that the relative magnitude of these terms are $\chi_{FIEE} > \chi_{IFI} \gg \chi_{IEE} \geq 0 \geq \chi_{IB}$. Acquiring the temperature dependence of each pairwise interac-

tion parameter, one general equation estimating the χ_{eff} for this system at any temperature and extent of fluorination was derived. Using the above information, a large portion of the experimental phase diagram has been mapped from only eight parent materials. The existence of lamellae, gyroid, and cylinders has been determined by SAXS, Interestingly, the gyroid phase is found to persist to unexpectedly strong degrees of segregation.

Acknowledgment. This work was supported by the MRSEC Program of the National Science Foundation under Awards DMR-9809364 and DMR-0212302. We thank Dr. R. Bernard Grubbs and Dr. Yu Ren for assistance with the modification chemistry and many helpful discussions. Joona Bang collected the SANS data. M.A.H. acknowledges DuPont for a Young Professor Grant and 3M for a nontenured faculty award.

References and Notes

(1) Lodge, T. P.; Pan, C.; Jin, X.; Liu, Z.; Zhao, J.; Maurer, W. W.; Bates, F. S. *J. Polym. Sci., Polym. Phys. Ed.* **1995**, *33*, 2289.
(2) Leibler, L. *Macromolecules* **1980**, *13*, 1602.
(3) Papadakis, C. M.; Almdal, K.; Mortensen, K.; Posselt, D. *Europhys. Lett.* **1996**, *36*, 289.
(4) Semenov, A. N. *Sov. Phys. JETP* **1985**, *61*, 733.
(5) Nyrkova, I. A.; Khokhlov, A. R.; Doi, M. *Macromolecules* **1993**, *26*, 3601.
(6) Semenov, A. N.; Nyrkova, I. A.; Khokhlov, A. R. *Macromolecules* **1995**, *28*, 7491.
(7) Gehlsen, M. D.; Bates, F. S. *Macromolecules* **1993**, *26*, 4122.
(8) Adams, J. L.; Quiram, D. J.; Graessley, W. W.; Register, R. A.; Marchand, G. R. *Macromolecules* **1998**, *31*, 201.
(9) Wang, S.-M.; Tsiang, R. C.-C. *J. Polym. Sci., Polym. Chem. Ed.* **1996**, *34*, 1483.
(10) Grubbs, R. B.; Broz, M. E.; Dean, J. M.; Bates, F. S. *Macromolecules* **2000**, *33*, 2308.
(11) McGrath, M. P.; Sall, E. D.; Tremont, S. J. *Chem. Rev.* **1995**, *95*, 381.
(12) Weiss, R. A.; Sen, A.; Pottick, L. A.; Willis, C. L. *Polym. Commun.* **1990**, *31*, 220.
(13) Szczubialka, K.; Ishikawa, K.; Morishima, Y. *Langmuir* **1999**, *15*, 454.
(14) Stone, V. W.; Jonas, A. M.; Legras, R.; Dubois, P.; Jerome, R. *J. Polym. Sci., Polym. Chem. Ed.* **1999**, *37*, 233.
(15) Wall, L. A., Ed. *Fluoropolymers*; Wiley-Interscience: New York, 1972.
(16) Ren, Y.; Lodge, T. P.; Hillmyer, M. A. *J. Am. Chem. Soc.* **1998**, *120*, 6830.
(17) Reisinger, J. J.; Hillmyer, M. A. *Prog. Polym. Sci.* **2002**, *27*, 971.
(18) Banks, R. E.; Smart, B. E.; Tatlow, J. C., Eds. *Organofluorine Chemistry: Principles and Commercial Applications*; Plenum Press: New York, 1994.
(19) Thomas, R. R. In *Fluoropolymers*; Hougham, G., Cassidy, P. E., Johns, K., Davidson, T., Eds.; Kluwer Academic/Plenum Publishers: New York, 1999; Vol. 2, p 47.
(20) Hillmyer, M. A.; Lodge, T. P. *J. Polym. Sci., Polym. Chem. Ed.* **2001**, *40*, 1.
(21) Matsen, M. W.; Bates, F. S. *Macromolecules* **1996**, *29*, 1091.
(22) Davidock, D. A.; Hillmyer, M. A.; Lodge, T. P. *Macromolecules* **2003**, *36*, 4682.
(23) Gilman, H.; Cartledge, F. K. *J. Organomet. Chem.* **1964**, *2*, 447.
(24) Ndoni, S.; Papadakis, C. M.; Bates, F. S.; Almdal, K. *Rev. Sci. Instrum.* **1995**, *66*, 1090.
(25) Halasa, A. F.; Lohr, D. F.; Hall, J. E. *J. Polym. Sci., Polym. Chem. Ed.* **1981**, *19*, 1357.
(26) Kang, J. W. The Firestone Tire & Rubber Company, U.S. Patent 3,993,885, 1975.
(27) Grubbs, R. B.; Dean, J. M.; Bates, F. S. *Polym. Mater. Sci. Eng.* **1999**, *81*, 153.
(28) Maynard, H. D.; Grubbs, R. H. *Tetrahedron Lett.* **1999**, *40*, 4137.
(29) Ren, Y.; Lodge, T. P.; Hillmyer, M. A. *Macromolecules* **2000**, *33*, 866.
(30) Bates, F. S.; Rosedale, J. H.; Bair, H. E.; Russell, T. P. *Macromolecules* **1989**, *22*, 2557.
(31) Fetters, L. J.; Lohse, D. J.; Richter, D.; Witten, T. A.; Zirkel, A. *Macromolecules* **1994**, *27*, 4639.
(32) March, J. In *Advanced Organic Chemistry: Reactions, Mechanisms, and Structure*, 4th ed.; J. Wiley and Sons: New York, 1992; pp 734−878.
(33) Hallman, P. S.; Evans, D.; Osborn, J. A.; Wilkinson, G. *Chem. Commun.* **1967**, 305.
(34) Hallman, P. S.; McGarvey, B. R.; Wilkinson, G. *J. Chem. Soc. A* **1968**, 3143.
(35) Jardine, I.; McQuillin, F. J. *Tetrahedron Lett.* **1968**, 5189.
(36) Roland, C. M. *Macromolecules* **1987**, *20*, 2557.
(37) Roland, C. M. *J. Polym. Sci., Polym. Phys. Ed.* **1988**, *26*, 839.
(38) Roovers, J.; Toporowski, P. M. *Macromolecules* **1992**, *25*, 3454.
(39) Tomlin, D. W.; Roland, C. M. *Macromolecules* **1992**, *25*, 2994.
(40) Trask, C. A.; Roland, C. M. *Macromolecules* **1989**, *22*, 256.
(41) Miller, J. B.; McGrath, K. J.; Roland, C. M.; Trask, C. A.; Garroway, A. N. *Macromolecules* **1990**, *23*, 4543.
(42) Cohen, R. E.; Ramos, A. R. *Macromolecules* **1979**, *12*, 131.
(43) Bates, F. S.; Bair, H. E.; Hartney, M. A. *Macromolecules* **1984**, *17*, 1987.
(44) Bandrup, J., Immergut, E. H., Grulke, E. A., Eds. *Polymer Handbook*, 4th ed.; John Wiley & Sons: New York, 1999.
(45) Hashimoto, T.; Shibayama, M.; Kawai, H. *Macromolecules* **1980**, *13*, 1237.
(46) Hadziioannou, G.; Skoulios, A. *Macromolecules* **1982**, *15*, 258.
(47) Ren, Y.; Lodge, T. P.; Hillmyer, M. A. *Macromolecules* **2002**, *35*, 3889.
(48) Flory, P. J. *Principles of Polymer Chemistry*; Cornell University Press: Ithaca, NY, 1953.
(49) Helfand, E.; Wasserman, Z. R. *Macromolecules* **1976**, *9*, 879.
(50) Bates, F. S.; Fredrickson, G. H. *Annu. Rev. Phys. Chem.* **1990**, *41*, 525.
(51) Matsen, M. W.; Bates, F. S. *Macromolecules* **1996**, *29*, 7641.
(52) Hamley, I. W. *The Physics of Block Copolymers*; Oxford University Press: Oxford, 1998.
(53) Equations for the lamellar, cylindrical, and spherical morphologies can be found in ref 63. Since we have no knowledge of a similar equation for the gyroid morphology, and since the use of the cylinder equation in place of the lamellae equation would not significantly affect the conclusions, we feel it is safer to employ a single expression for χ.
(54) Hillmyer, M. A.; Bates, F. S.; Almdal, K.; Mortensen, K.; Ryan, A. J.; Fairclough, J. P. A. *Science* **1996**, *271*, 976.
(55) Hajduk, D. A.; Ho, R.-M.; Hillmyer, M. A.; Bates, F. S.; Almdal, K. *J. Phys. Chem. B* **1998**, *102*, 1356.
(56) Mark, J. E., Ed. *Physical Properties of Polymers Handbook*; American Institute of Physics: Woodbury, NY, 1996.
(57) Bates, F. S.; Rosedale, J. H.; Fredrickson, G. H. *J. Chem. Phys.* **1990**, *92*, 6255.
(58) Boothroyd, A. T.; Rennie, A. R.; Wignall, G. D. *J. Chem. Phys.* **1993**, *99*, 9135.
(59) ten Brinke, G.; Karasz, F. E.; MacKnight, W. J. *Macromolecules* **1983**, *16*, 1827.
(60) Kambour, R. P.; Bendler, J. T.; Bopp, R. C. *Macromolecules* **1983**, *16*, 753.
(61) Paul, D. R.; Barlow, J. W. *Polymer* **1984**, *25*, 487.
(62) The volume fraction of the PEE segment in the block copolymers (f_{PEE}) decreases slightly with increasing extent of difluorocarbene modification. The volume fractions can be calculated from the chemical degree of polymerization of each component, the molecular weight of each component (M_0 = 56, 68, and 118 g/mol for EE, I, and FI, respectively), and the room temperature densities. Again, the temperature dependence was ignored. The greatest change occurs for a nearly symmetric block copolymer, where the composition is found to decrease from $f_{PEE} = 0.529$ for the hydrogenated precursor to $f_{PEE} = 0.472$ upon complete difluorocarbene modification. At more asymmetric compositions, the change is not as significant.
(63) Matsen, M. W.; Bates, F. S. *J. Chem. Phys.* **1997**, *106*, 2436.
(64) Matsen, M. W.; Bates, F. S. *J. Polym. Sci., Polym. Phys. Ed.* **1997**, *35*, 945.
(65) Fredrickson, G. H.; Helfand, E. *J. Chem. Phys.* **1987**, *87*, 697.
(66) Fredrickson, G. H. *Macromolecules* **1987**, *20*, 2535.
(67) Anastasiadis, S. H.; Russell, T. P.; Satija, S. K.; Majkrzak, C. F. *Phys. Rev. Lett.* **1989**, *62*, 1852.
(68) Anastasiadis, S. H.; Russell, T. P.; Satija, S. K.; Majkrzak, C. F. *J. Chem. Phys.* **1990**, *92*, 5677.
(69) Menelle, A.; Russell, T. P.; Anastasiadis, S. H.; Satija, S. K.; Majkrzak, C. F. *Phys. Rev. Lett.* **1992**, *68*, 67.

(70) Karim, A.; Singh, N.; Sikka, M.; Bates, F. S.; Dozier, W. D.; Felcher, G. P. *J. Chem. Phys.* **1994**, *100*, 1620.
(71) Podariu, I.; Chakrabarti, A. *J. Chem. Phys.* **2003**, *118*, 11249.
(72) Wang, J.; Mao, G.; Ober, C. K.; Kramer, E. J. *Macromolecules* **1997**, *30*, 1906.
(73) Lodge, T. P.; Hamersky, M. W.; Hanley, K. J.; Huang, C.-I. *Macromolecules* **1997**, *30*, 6139.
(74) Higgins, J. S.; Benoît, H. C. *Polymers and Neutron Scattering*; Clarendon Press: Oxford, England, 1994.
(75) Hanley, K. J.; Lodge, T. P. *J. Polym. Sci., Polym. Phys. Ed.* **1998**, *36*, 3101.
(76) Hanley, K. J.; Lodge, T. P.; Huang, C.-I. *Macromolecules* **2000**, *33*, 5918.
(77) Förster, S.; Khandpur, A. K.; Zhao, J.; Bates, F. S.; Hamley, I. W.; Ryan, A. J.; Bras, W. *Macromolecules* **1994**, *27*, 6922.
(78) Khandpur, A. K.; Förster, S.; Bates, F. S.; Hamley, I. W.; Ryan, A. J.; Bras, W.; Almdal, K.; Mortensen, K. *Macromolecules* **1995**, *28*, 8796.
(79) Zhao, J.; Majumdar, B.; Schulz, M. F.; Bates, F. S.; Almdal, K.; Mortensen, K.; Hajduk, D. A.; Gruner, S. M. *Macromolecules* **1996**, *29*, 1204.
(80) Hajduk, D. A.; Takenouchi, H.; Hillmyer, M. A.; Bates, F. S.; Vigild, M. E.; Almdal, K. *Macromolecules* **1997**, *30*, 3788.
(81) Hamley, I. W.; Fairclough, J. P. A.; Ryan, A. J.; Mai, S. M.; Booth, C. *Phys. Chem. Chem. Phys.* **1999**, *1*, 2097.
(82) Vigild, M. E.; Almdal, K.; Mortensen, K.; Hamley, I. W.; Fairclough, J. P. A.; Ryan, A. J. *Macromolecules* **1998**, *31*, 5702.
(83) Wang, C.-Y.; Lodge, T. P. *Macromolecules* **2002**, *35*, 6997.

MA035248Y